
SAE Aero Design® East 2001

University of Maryland
Team #30
“Dragonfly”



EXECUTIVE SUMMARY

To SAE Aero Design® Officials:

Enclosed is our design report pertaining to our radio-controlled aircraft entry, The Dragonfly, into the SAE Aero Design® East 2001 Competition. This report includes the design options we considered before settling on our final design. It then outlines the reasons for our final choice and a description of each component's governing aspects. Our production methods of each component are to follow, and our testing procedures are then described. Finally, CAD drawings of the integrated plane are included.

Our final design is a span loading configuration with tail dragger landing gear and a conventional tail. Mounting the weight box along the length of the wing has eliminated the need for a fuselage. From data reduction, the predicted payload that we expect to carry is 22 pounds.

Sincerely,

University of Maryland Heavy Lift Design Team

Team 30

TABLE OF CONTENTS

EXECUTIVE SUMMARY.....	ii
INTRODUCTION.....	1
CONCEPT GENERATION.....	1
WING DESIGN.....	3
TAIL DESIGN.....	7
LANDING GEAR.....	9
ENGINE MOUNT.....	10
INTEGRATION.....	11
PERFORMANCE ESTIMATION.....	12
COST ANALYSIS.....	17
MASS AND BALANCE.....	17
WIND TUNNEL TESTING.....	19
LANDING GEAR TESTING.....	20
FLIGHT TESTING.....	21
CONCLUSION.....	22
REFERENCES.....	23

INTRODUCTION

The University of Maryland's Dragonfly is a model-scale aircraft designed to lift a heavy payload in the Society of Automotive Engineers' Aero Design 2001 competition. The design of this aircraft was dictated by the contest regulations, including engine size, payload volume, maximum planform area, and maximum take-off and landing ground roll.

In light of the restrictions on the design, the University of Maryland design team has chosen an unconventional span-loader design, in which the payload is carried in the wing of the aircraft. This design uniquely fulfills the requirements of the competition. First, it allows the payload distribution to be approximately equal to the lift distribution, which reduces the amount of internal structure needed to provide load-transfer paths between the lifting surfaces and the payload. Secondly, it eliminates the fuselage, reducing drag. The elimination of the fuselage provides more planform area to be used for the wings within the specified design limitations. The span-loader design is predicted to lift a 22-pound (lb.) payload at standard sea level.

CONCEPT GENERATION

Our concept generation was geared towards satisfying the requirements imposed by the Aero Design® East rules. For the overall design, these requirements were:

- Minimum payload of 8 pounds
- Maximum planform area of 1200 in²
- Maximum take off distance of 200 ft.
- Maximum landing distance of 400 ft.
- Controllability during flight.
- Structural integrity

Several concepts took shape during the initial design phase. To satisfy the payload requirements, an airfoil was selected that would perform well under the low Reynolds number conditions at which the plane would be flown. In order to minimize the wetted area, which generates a considerable amount of drag, the fuselage was eliminated. The payload would be carried inside the wing, so the need for a thick airfoil was important in the airfoil selection process. Once the appropriate airfoil was selected, the geometry of the wing was chosen to give the best flight performance at the lowest design and manufacturing cost. Calculations, which will be described later, showed that taper ratio provided no benefit. The wing planform area and the wingspan drove the wing aspect ratio selection. For ease of manufacturing, the decision was made to keep the wing untwisted and unswept. In order for ground roll to occur at an angle yielding the maximum lift coefficient, the wing angle of incidence was chosen to be 9-10°.

To address the issue of static stability of the airplane, several choices were considered, such as the use of canard versus a conventional tail arrangement. The canard provides a more efficient use of lift and better stall recovery characteristics, but is unfavorable due to control and stability concerns and spoiled flow over the main wing. Therefore, a conventional tail configuration was selected.

The options for the landing gear configurations were numerous; quadricycle, bicycle, tricycle and tail dragger configurations were considered. Despite their increased stability during ground roll, the quadricycle and bicycle configurations were associated with a significant weight and drag penalty. The tricycle and tail dragger configurations reduced weight and drag. The tricycle configuration required an extended front wheel that would have interfered with the propeller, so that option was eliminated. The tail dragger configuration was chosen in order to

minimize the risk of hitting the propeller during takeoff and landing, and the necessity to have the wing close to $C_{L_{max}}$ during ground roll.

The stability and balance criteria favored a puller engine. By locating the engine ahead of the main wing leading edge, the center of gravity of the body wing combination was shifted forward, closer to the aerodynamic center.

The final concept could be described in a few words as a flying wing with an extended tail boom on the back for stability and balance, and an engine located ahead of the leading edge.

WING DESIGN

The airfoil is arguably the most important element of a good wing design. Airfoil data for high-Reynolds number applications is widely available, dating back to the original NACA tests 70 years ago. However, airfoil performance changes dramatically at low Reynolds numbers ($Re < 300,000$), such as would be found on a model-scale wing operating in typical atmospheric conditions. Data for low-Reynolds number airfoils are rare, a large portion of it having been produced under Dr. Michael Selig's low-speed airfoil program at the University of Illinois at Urbana-Champaign.

For this wing design, Dr. Selig's *Summary of Low-Speed Airfoil Data* was consulted, and the classic FX 63-137 was chosen for its superior low Reynolds number characteristics and the ability to accommodate a large internal bay. As long as the Reynolds number was kept above 100,000, this airfoil has been shown to produce a maximum lift coefficient higher than 1.5, whereas conventional airfoils are known to degrade well below this level at low Reynolds numbers.

Figure 1 shows the FX 63-137 airfoil. Note the resemblance to a supercritical airfoil; at low Reynolds numbers, the flow is primarily laminar and must not be allowed to separate early. Also, this airfoil is observed to have a flap-like trailing edge, suitable for high-lift applications.

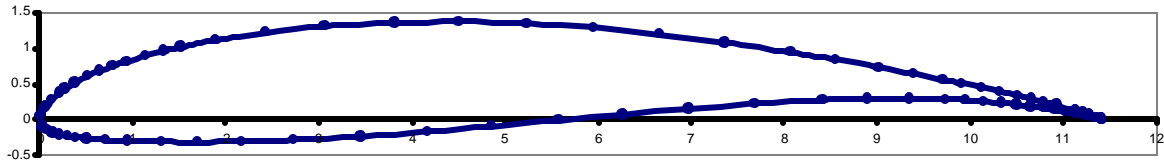


Figure 1. FX 63-137 Low-speed Airfoil

Airfoil selection was followed by wing design. Having decided previously to pursue a span-loading design for the aircraft, the next step was to design a suitable wing. Several factors considered were aspect ratio, wingspan, weight box span, taper ratio, dihedral and extra high-lift devices. The first four parameters were calculated by examining geometric constraints and traditional airfoil theory. Due to their empirical nature, dihedral and high-lift devices were not analyzed.

The geometric parameters were determined after an airfoil was chosen. First, the airfoil shape was plotted from data in *Selig et al.* Because a span-loading design was chosen, it was important to integrate the weight box into the wing and determine the weight box dimensions early on. Minimum weight box volume was specified in the regulations, so it was only necessary to determine the cross-sectional area based on the airfoil shape and chord length. To decouple pitching moment and payload weight, it was decided to center the weight box about the airfoil quarter-chord. Based on this assumption, numerous possible weight box cross-sections were drawn inside the original airfoil plot. The cross-section yielding the largest area was chosen from this trial-and-error process. After many drawings, the best height and width of the box

were found to be $0.075c$ and $0.3875c$, respectively, where c is the chord of the airfoil. (Due to practical limitations during construction, the weight box center of gravity is slightly aft of the wing quarter-chord.)

Next, taper ratio was examined. A high taper ratio would give the wing more of an elliptical lift distribution, thus increasing the Oswald efficiency factor. However, a taper ratio would also force the weight box span to be shorter relative to the total wingspan (Fig. 2).

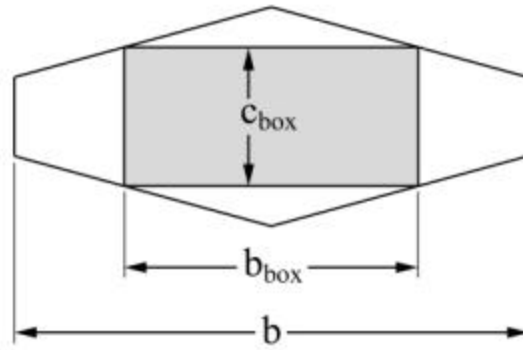


Figure 2. Tapered Wing with Weight Box

The geometric relationship between aspect ratio AR , taper ratio I and weight box span \bar{b} (normalized with respect to wingspan) is

$$\bar{b}^2(I-1)^2 + 2\bar{b}^2(I-1) + \bar{b} = \frac{V_{box}(1+I)^2\sqrt{SAR}}{.116S^2} \quad (1)$$

From conventional wing theory and Equation 1, it is possible to note the effects of wing taper on weight box span and wing efficiency (Fig. 3). Clearly, a taper ratio of 1 (no wing taper) is most desirable; for non-zero taper, the weight box volume requirement severely limits aspect ratio. Efficiency is dominated by aspect ratio, therefore large aspect ratio is more important than wing taper.

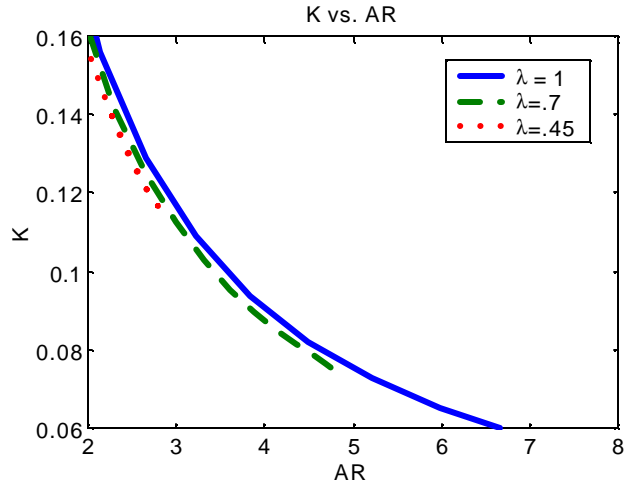


Figure 3. Efficiency, Aspect Ratio and Taper Ratio

For structural reasons, the aspect ratio was limited to 8, fixing the weight box span ratio at 0.86. The full set of wing dimensions is given in Table 1.

Aspect Ratio	8
Planform area (in ²)	1014.6
Wingspan (in)	89
Chord (in)	11.4
Thickness (in)	1.56
Taper ratio	1
Weight box volume (in ³)	300
Weight box span (in)	79.27
Weight box height (in)	0.86
Weight box width (in)	4.43

Table 1. Wing and Weight Box Geometry

The wing was constructed from a foam core and fiberglass skin. A hot wire cutting process was used to shape the foam. Two spars span a portion of the wing in the vicinity of the landing gear forward and aft of the weight box.

After the foam core was shaped, it was covered with a pre-impregnated fiberglass composite material in a manual lay-up process. One ply of fiberglass was used over the entire core with a second ply reinforcing the high-stress area.

The foam core was removed from the wing in the portion of the wing where the weight box was to be placed. Two spars were fabricated using Graphite Epoxy composite material. These spars were mounted within the wing flanking the weight box as shown in Figure 4. Their purpose is to provide bending stiffness and to keep the weight box securely in place. In addition, the spars will absorb and distribute the load from the landing gear upon landing. The box was placed between the spars close to the quarter chord.

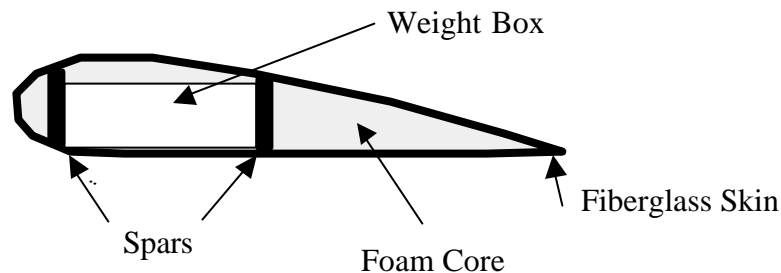


Figure 4. Wing Cross-Section

TAIL DESIGN

Once the wing dimensions had been determined, a tail was designed that provided adequate stability and control of the aircraft.

A conventional configuration was chosen for the tail of the aircraft. This design has the lightest structure compared with other configurations. The conventional tail will also keep the

control surfaces from being blanketed by the downwash from the wing. The tail boom was mounted at 4.5 degrees above the chord of the main wing, so the low horizontal tail will ensure that the elevator is below the wing wash near stall conditions, and to allow for a sufficient angle of attack at take off.

In order to determine the boom length of the tail, the horizontal and vertical volume coefficients of the tail were chosen to be 0.45 and 0.03, respectively. These values are based on historical data. The planform area of the horizontal tail, S_{HT} , was decided to be 10 percent of the total allowed planform area, or 120 square inches. From the wing design, it was known that the aspect ratio, AR , is 8, the wing planform, S_W , is 87 percent of the total planform, or 1044 square inches, the chord length, C , is 11.4 inches, and the wingspan, b , is 91.4 inches.

The length from the intersection of the mean aerodynamic chord and the quarter chord of the wing and the intersection of the mean aerodynamic chord and the quarter chord of the tail is

$$L = V_{HT} C S_W / S_{HT} \quad (3)$$

This length is calculated to be 44.7 inches.

The area of the vertical tail is then calculated:

$$S_{VT} = V_{VT} b S_W / L \quad (4)$$

This area is found to be 64 square inches.

Other dimensions of the tail were based on historical data. The sweep of the horizontal tail is 5 degrees, and the sweep of the vertical tail is 40 degrees. The aspect ratio of the horizontal tail is 4 and the aspect ratio of the vertical tail is 1.5. The taper ratio of the horizontal and vertical tails is 0.4.

The horizontal and vertical tails are both constructed with 1/8-inch thick balsa wood sandwiched between two plies of fiberglass. These two pieces are attached with epoxy. The

vertical tail is inserted into a slot in the Kevlar tail boom and attached with bolts through the vertical tail. A number of holes are drilled in the vertical tail to allow the tail angle of attack to be adjusted.

LANDING GEAR

The Dragonfly uses tail-dragger landing gear, a configuration that is particularly suited to the span loader design of the aircraft. First and foremost, this configuration allows the main gear to be attached directly to the wing, transferring most of the landing loads into the internal structure. More specifically, the main gear is connected through hard points to internal graphite wing spars. These spars are used to stiffen the wing and to connect the separately-manufactured wing halves, making this design quite efficient. Also, the tail wheel eliminates the need for attaching a cumbersome nose wheel to our fuselage-less design, instead allowing a steerable tail wheel to be directly linked to the rudder.

The main gear is 10-ply Kevlar-epoxy composite with a balsa wood core. The composites provide a high degree of strength with a minimum of weight, while the balsa core increases bending stiffness. The gear is also fitted with tension wires to provide additional support during landing and ground-roll. These wires are strung from the inside of each wheel to attachment points on the opposite strut to prevent splaying under high loads. This design has withstood repeated runs on the landing gear test rig while loaded with 30 pounds of weight and high yaw angles.

The tail wheel was epoxied to the underside of the horizontal stabilizer and attached to the rudder through a strut imbedded in the rudder. This allowed the tail wheel to be steered using the rudder control.

ENGINE MOUNT

The engine mount was made of 1/4-inch aluminum plate attached to the hard point near the leading edge of the airplane. The aluminum was bent to align the engine with the top surface of the aircraft. The front of the engine mount was machined to make a bracket to hold the engine. Sections were machined out of the aluminum to reduce the weight.

To carry the tension and some of the torsional loads, 1/8-inch aluminum straps were bolted to the main piece of the mount and the hard points forward and aft of the weight box. These straps also carry the compression on the top of the wing that occurs under certain conditions (such as landing).

To balance the weight of the tail, the engine was mounted on top of the brackets about 14 inches forward of the leading edge with the fuel tank placed aft of the engine. The space where the main piece of the engine mount joins with the straps is used to hold the receiver and the battery. A rough sketch of the engine mount is shown below:

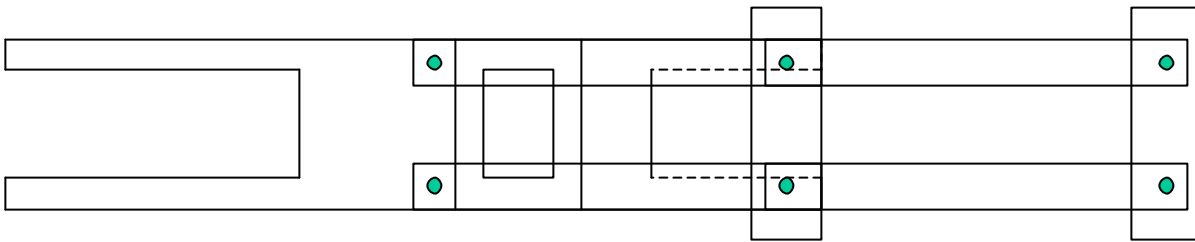


Figure 5. Top View of Engine Mount

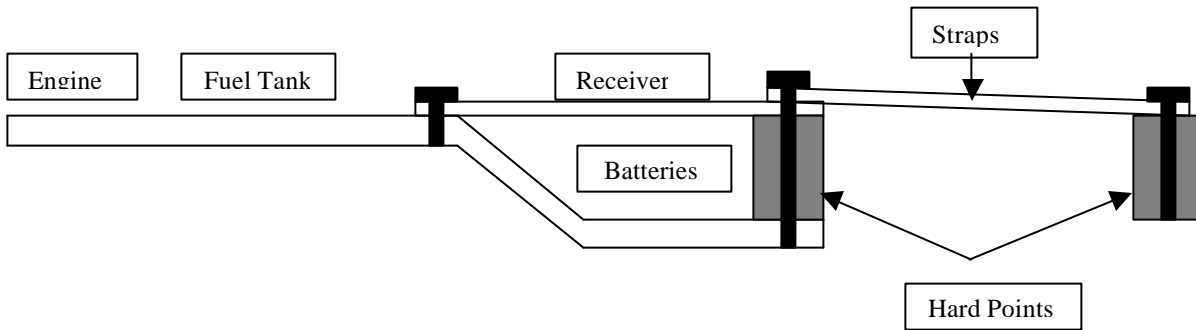


Figure 6. Side View of Engine Mount

INTEGRATION

There were several important considerations for the integration of the aircraft: weight and aerodynamics, structural integrity, and ease of access to the weight box.

Early in the design process, it was decided to have a weight box located inside the wing. The weight box spanned 80% of the wingspan to allow some freedom for changing the wing tips. A removable panel immediately above the weight box was cut into the upper skin. Because the landing gear is on the lower surface of the wing, it was decided that the panel should be on the upper surface of the wing. This allowed for the easiest loading, easiest fabrication of the cavity, and did not interfere with associated structure, such as wing spars.

A bracket was designed to mount the engine onto the wing. Since this connection had to be very strong to withstand the vibrational and longitudinal loads of the engine and to carry a strong moment, it was decided that the bracket should be permanently attached to the airplane. The engine bracket was designed to attach at the top and bottom of the leading edge of the wing, with two removable bars that run back from the leading edge to behind the weight box. These bars help to restore some of the strength that was lost by cutting the panel from the top skin.

It was desired that the servos controlling the airplane should be imbedded in the wing to produce the least amount of drag. This was done for the flaperon controls; however, because of

the way in which the tail boom attached to the rest of the airplane, this was impossible for the tail controls. The servos for the tail were located at the base of the tail boom, with control rods running through the boom aft to the tail. Small holes were drilled into the tail boom, to allow the control rods to come through, and attach to the servos. This configuration kept the weight forward, helping with the balance of the airplane.

The other components that were considered were the fuel tank, radio receiver, battery pack, and throttle servo. Because the engine-mounting bracket was so long, it was possible to put these four components on the bracket. The throttle servo was the most forward in this group, being placed just aft the engine on the starboard side of the mount. The fuel tank was placed directly aft of the servo, with the receiver and battery pack located aft of the fuel tank. This configuration kept the fuel tank and throttle servo close to the engine. Placing the components directly behind the engine helped keep their weight forward, without increasing the frontal area of the airplane.

PERFORMANCE ESTIMATION

Takeoff distance and maximum takeoff weight were the two main design considerations for this Aero Design aircraft. Accordingly, it was important to develop an understanding of the aircraft's predicted takeoff performance under different loading and wind conditions. Having chosen the major wing and tail parameters, it was possible to develop a differential equation describing the takeoff roll based on the chosen parameters and some historical data. This differential equation was then solved numerically for different takeoff scenarios, yielding a series of maximum gross takeoff weights. The aircraft's empty weight was subtracted to yield

maximum payload weight, and a correction factor was subtracted from this figure to give a realistic prediction for payload weight.

The wing is the most important factor affecting takeoff performance. Accordingly, derivation of the takeoff equation began with an understanding of the wing and airfoil. From the FX 63-137 airfoil data given in Selig et.al, the lift curve was plotted at a Reynolds number of 200,000 (Fig. 7).

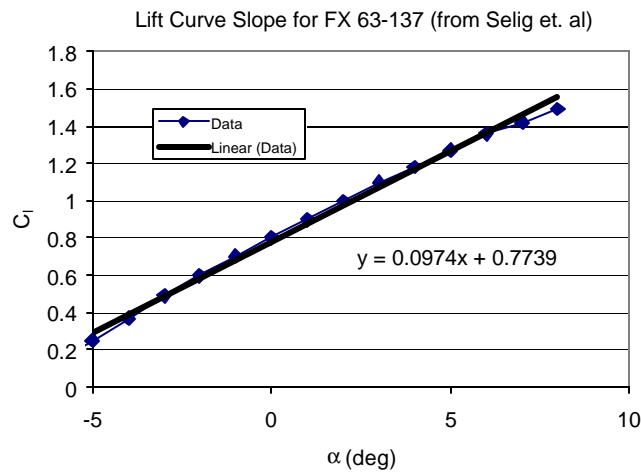


Figure 7. Lift Curve Slope for FX 63-137

The lift curve slope was determined from this data, and further calculations assumed a takeoff angle of attack of 10° .

This information was used to write the equation of motion during takeoff. Considering such factors as constant thrust (appropriate at low speeds), headwind, ground effect, drag due to rolling friction and drag due to aerodynamic forces, the equation of motion can be written as

$$m\ddot{x} + \frac{1}{2} r_\infty S (c_d + KC_L^2 - m_{rolling} C_L) (\dot{x} + V_{wind})^2 + m_{rolling} W - T_{max} = 0 \quad (5)$$

The zero-lift drag coefficient was determined from experimental wind tunnel data, and all other values were based on theory or historical data.

This non-linear differential equation could be manipulated and an approximate solution determined analytically, but such a process was unnecessary. Instead, Matlab was used to solve the equation numerically and determine the resulting ground roll time history. The graphical results of this analysis are given in Figs. 8-10, where ground roll is plotted as a function of takeoff weight for various wind conditions. It was possible to determine the maximum takeoff weight by drawing a line through the 200-foot mark, the longest allowable takeoff roll.

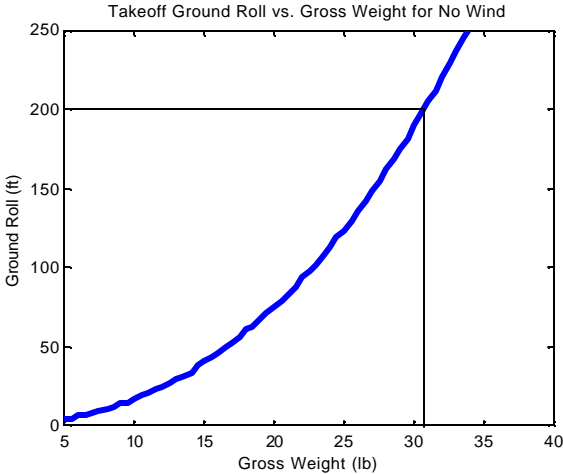


Figure 8. Ground Roll Without Wind

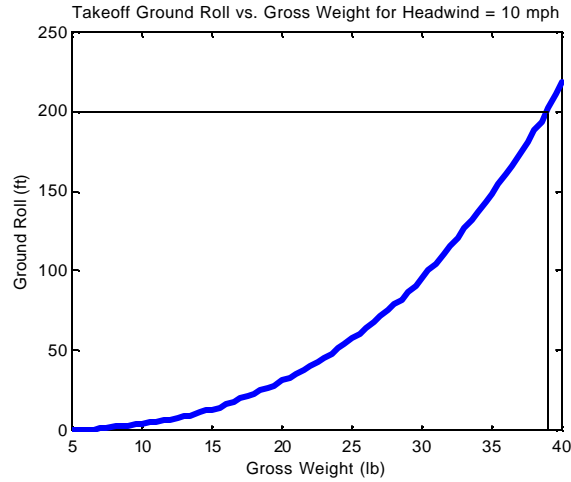


Figure 9. Ground Roll with Headwind of 10 mph

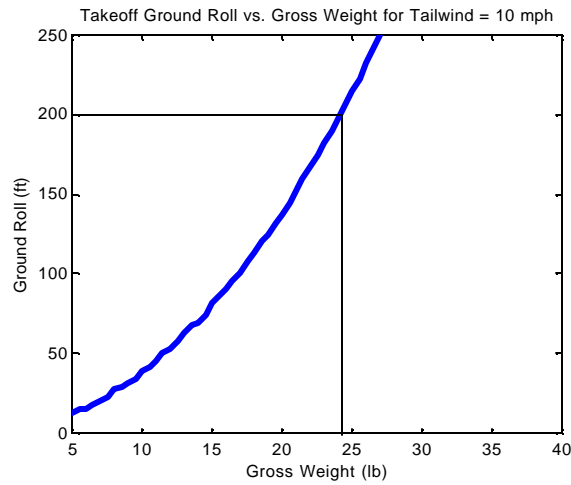


Figure 10. Ground Roll with Tailwind of 10 mph

Table 2 lists the numerical takeoff performance estimates for no wind, a headwind, and a tailwind. It is predicted that the maximum gross weight can be 30.5 pounds for zero wind, although a tailwind will severely diminish performance. Assuming an empty weight of 7.5 pounds (based on experimental data), this performance estimate calls for a 23-pound maximum payload at standard sea level.

Headwind (mph)	0	10	-10
Gross Weight (lb)	30.5	39	24
Takeoff Speed (ft/s)	49.6	56.0	44.0
C_l	1.44	1.44	1.44
C_d	0.118	0.118	0.118
K	0.038	0.038	0.038
L/D	10.6	10.6	10.6
α (deg)	10	10	10

Table 2. Takeoff Parameters

University of Maryland: Dragonfly
Payload Weight vs. Density Altitude

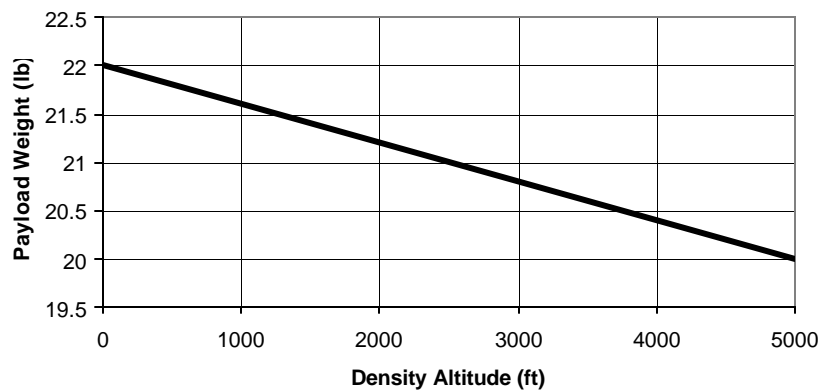


Figure 11. Predicted Payload Weight vs. Density Altitude

However, this estimate was based on ideal conditions and a flap-less wing. Flight-testing has revealed that 20 degrees of flaperons can significantly improve takeoff performance, but specific data are unavailable. Also, the analytical performance estimate was based on ideal conditions, suggesting a lower real-world performance estimate. In the end, all of these factors were considered in addition to past experience, and the final maximum predicted payload weight was

qualitatively fixed at 22 pounds at standard sea level. Density altitude correction was determined by varying density in Equation 5 and performing a linear fit to the results.

COST ANALYSIS

As shown in Table 3, a single production of The Dragonfly is estimated to cost \$1774.

Items	Rate	Quantity	<u>Cost</u>
Fiberglass*	\$4/ft ²	36ft ²	\$144
Vacuum Bagging**			\$200
Foam Core	\$11/package	1 package	\$11
Autoclave	\$60/hr	10 hrs	\$600
Nitrogen Tank	\$12/tank	6 tanks	\$72
Salary for Research Engineer	\$45/hr	1 hr	\$45
Aluminum Weight Box	\$80 each	1	\$80
Engine (O.S. .61 FX)	\$160 each	1	\$160
6-channel radio, 5 servos and receiver	\$300/kit	1	\$300
4 oz. Fuel Tank	\$4 each	1	\$4
Graphite	\$8/ft ²	1	\$8
Miscellaneous (wheels, landing gear struts, aluminum engine mount and hardware)			\$150
Total Cost			\$1774

* Including wing, horizontal tail, vertical tail and boom

** Flat Rate

Note: All costs are estimates. This cost analysis is for a single airplane. Extra costs are expected for spare parts.

Table 3. Cost Analysis

MASS AND BALANCE

The aircraft was designed for the center of gravity to coincide as closely as possible with the quarter chord of the wing. The center of gravity of the weight box assembly is also located nearly at the quarter chord, so as to remove any significant weight-dependent pitching moment.

The quarter chord of the wing is located 2.85 inches (in.) aft of the leading edge of the wing. Based on this initial estimation, the moments due to the various components of the aircraft were calculated about the center of gravity. The moments were summed to give a net value of the pitching moment about the center of gravity. The moment contribution due to each component is tabulated in Table 3. The locations are measured between the center of gravity of the aircraft and center of gravity of each component.

Components Forward of C.G.	Weight	Arm
Propeller	0.088	16.75
Engine	1.62	13.92
Fuel tank	0.32	9.92
Electronics	0.56	8
Engine mount	0.84	7.87
	Total Moment	38.38

Components Aft of C.G.	Weight	Arm
Tail	0.99	38.55
	Total Moment	38.33

Table 4. Summation of Moments About Center of Gravity

The pitching moment can be calculated by

$$\text{Pitching Moment} = \Sigma M_{\text{aft}} - \Sigma M_{\text{Forward}} = -0.05 \text{ lb-in.} \quad (6)$$

Thus, the airplane is slightly nose-heavy at the design payload weight, resulting in static stability.

WIND TUNNEL TESTING

Wind tunnel tests were conducted at the University of Maryland Glenn L. Martin Wind Tunnel in order to determine the most efficient wing tip design, to get an accurate estimate for zero lift drag, C_{D0} , and to validate the theoretical lift to drag ratio.

Three different wing tip configurations were examined – blunt tip, endplates, and Hoerner tips. The lift to drag ratio of the blunt tip configuration was 9.2, and subsequent testing of both endplates and Hoerner tips showed an improvement in lift over drag of 9.4 for the endplates and 9.5 for the Hoerner tips. The Hoerner tips were most beneficial and are included on the final design.

Using lift and drag coefficients determined from experimental data, zero lift drag was calculated from

$$C_D = C_{D,0} + K C_L^2 \quad (7)$$

The value for ‘K’ was taken to be .0381, which was based on historical data for aircraft of similar aspect ratio.

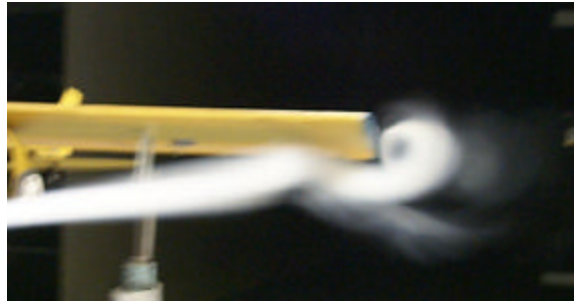


Figure 12: Wingtip Vortices at $\alpha = 10^\circ$

Additionally, the wind tunnel tests demonstrated the effectiveness of inclining the tail boom above the extended chord line of the wing. Indeed, this tactic causes the tail to lie outside of the wing downwash region (Fig. 13).



Figure 13: Wing Downwash

LANDING GEAR TESTING

The landing gear's strength and performance were examined using a custom test rig. The rig (Fig. 14), simulated the landing pattern with the plane landing at some angle of descent, and it simulated any side force that could occur upon landing.

A variable weight was attached to the landing gear structure. The mass was attached to two cords with variable slope, and then allowed to slide down the cords. Varying the slope of the cord changed the landing gear impact velocity and angle. This way, a broad range of landing speed and glide slope possibilities were simulated. A sideways impact simulation was included to address the concern of an unexpected crosswind before the plane touches the runway. To accomplish this, the weight box was initially mounted to the cords at a specified yaw angle with respect to the runway, ranging from 0 degrees for minimum sideway force to 90 degrees for the maximum sideway impact. To ensure strength of the landing gear assembly, the tests were performed from the ideal scenario (no crosswind, and minimum vertical speed), to the worst-case scenario (maximum crosswind, and maximum vertical speed) until failure of the components

occurred. The failed components were then strengthened and re-tested, until a high level of confidence was achieved.

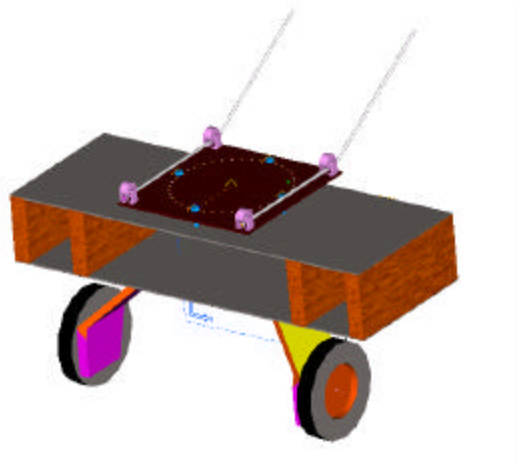


Figure 14: Landing Gear Test Rig

FLIGHT TESTING

Flight-testing of the initial design was useful in identifying a few balance and structural problems. The first flights were done with only the weight box (a payload of about six pounds). These flights revealed that the aircraft was slightly tail-heavy (due to inaccurate weight estimates during initial design). Ballast was used to restore proper balance. In subsequent designs, more accurate weight information was used to move the engine mount and weight box forward to achieve static stability.

As payload weight increased, weak points in the structural design were identified. The attachment between the tail wheel and the rudder was not strong enough, and subsequent designs had a more solid connection.

The original landing gear was not sturdy enough to handle extreme loading, in which large side forces were experienced. Newer designs have a balsa wood core that extends the

whole length of the gear and more Kevlar plies. A wire connecting the two wheels was added to keep the gear from spreading out when subjected to a heavy load.

CONCLUSION

The challenge presented by the SAE Aero Design Lift competition is a unique one in that the aircraft will be operating at a very specific flight condition; namely, to carry the greatest possible weight with a given amount of power. The ramifications of this requirement are seen throughout the aircraft's final design. After considering a multitude of designs and variations, a span-loading design with no fuselage was chosen in order to minimize the drag and structural weight. The rest of the aircraft was built around that configuration: a conventional tail to avoid disturbed flow from the wing and a tail dragging landing gear to avoid interference with the propeller and minimize weight.

The final product is predicted to lift 22 pounds at sea level density altitude.

REFERENCES

- 1) Anderson, John D. *Introduction to Flight*. New York: McGraw-Hill. 2000.
- 2) Raymer, Daniel P. *Aircraft Design: A Conceptual Approach*. Virginia: American Institute of Aeronautics and Astronautics. 1999.
- 3) Selig, Michael S., James J. Guglielmo, Andy P. Broeren, Philippe Giguère. *Summary of Low-Speed Airfoil Data*. Virginia: SoarTech Publications. 1995.
- 4) *University of Maryland SAE Heavy Lift Aero Design Fall 1999 Status Report*.
- 5) *2001 Aero Design East and 2001 Aero Design West Official Rules*.